

Unveiling quantum steering by quantum-classical uncertainty complementarity

Kuan-Yi Lee^{1,2,*}, Jhen-Dong Lin^{1,2,*}, Karel Lemr^{3,†}, Antonín Černoch⁴, Adam Miranowicz^{5,6}, Franco Nori^{5,7,8}, Huan-Yu Ku^{9,‡}, and Yueh-Nan Chen^{1,2,5,10,§}

¹Center for Quantum Frontiers of Research and Technology (QFort), National Cheng Kung University, Tainan 701, Taiwan

²Department of Physics, National Cheng Kung University, Tainan 701, Taiwan

³Palacký University in Olomouc, Faculty of Science, Joint Laboratory of Optics of Palacký University and Institute of Physics AS CR, 17. listopadu 12, 771 46 Olomouc, Czech Republic

⁴Institute of Physics of the Academy of Sciences of the Czech Republic, Joint Laboratory of Optics of Palacký University and Institute of Physics AS CR, 17. listopadu 50a, 772 07 Olomouc, Czech Republic

⁵Theoretical Quantum Physics Laboratory, Cluster for Pioneering Research, RIKEN, Wakoshi, Saitama 351-0198, Japan

⁶Institute of Spintronics and Quantum Information, Faculty of Physics, Adam Mickiewicz University, 61-614 Poznań, Poland

⁷Center for Quantum Computing, RIKEN, Wakoshi, Saitama 351-0198, Japan

⁸Department of Physics, The University of Michigan, Ann Arbor, 48109-1040 Michigan, USA

⁹Department of Physics, National Taiwan Normal University, Taipei 11677, Taiwan

¹⁰Physics Division, National Center for Theoretical Sciences, Taipei 106319, Taiwan

*These authors contributed equally

†k.lemr@upol.cz

‡huan.yu@ntnu.edu.tw

§yuehnan@mail.ncku.edu.tw

ABSTRACT

One of the remarkable aspects of quantum steering is its ability to violate local uncertainty complementarity relations. In this vein of study, various steering witnesses employing different uncertainty relations have been developed including Reid's criteria. Here, we introduce a novel complementarity relation between system's quantum and classical uncertainties corresponding to the distillable coherence and the von-Neumann entropy, respectively. We demonstrate a superior steering detection efficiency compared to an entropic uncertainty relation. Notably, our proposed steering witness can detect "all pure entangled states," while the entropic uncertainty relation cannot. We also experimentally validate such a property through a photonic system. Furthermore, a deeper connection to the uncertainty principle is revealed by showcasing the functionality of our proposed complementarity as a quantifier of measurement incompatibility and quantum steerability under genuine incoherent operations. Our work establishes a clear quantitative and operational link between coherence and steering, which are significant resources of quantum technologies, and underscores our efforts in bridging the uncertainty principle with quantum coherence.

Introduction

Quantum steering¹, as a type of quantum correlations that is classified between Bell nonlocality and quantum entanglement, has garnered significant attention due to its applications in one-sided device-independent quantum information processing²⁻⁶, including quantum random number generation^{7,8}, quantum key distribution^{9,10}, quantum metrology^{11,12}, and thermodynamics^{13,14} (see also recent reviews¹⁵⁻¹⁷). In addition, it exhibits a profound connection to the local uncertainty principle. In its original formulation, known as Reid's criteria^{18,19}, quantum steering is characterized by violating the Robertson-Schrödinger uncertainty relation. To date, the notion of characterizing quantum steering by its ability to violate uncertainty relation has been generalized to different forms, including the entropic uncertainty relation (EUR)²⁰⁻²³, the complementarity of coherence for mutually unbiased bases^{24,25}, metrological complementarity¹¹, etc. Moreover, a resemblance between quantum steering and measurement incompatibility has been uncovered²⁶⁻³¹, further refining our understanding of the connection

between steering and a generalized uncertainty principle.

In contrast to previous studies that focused on the uncertainty trade-offs between conjugated variables, recent works have examined different sources of uncertainty by separating the measured uncertainty into its quantum and classical components^{32–36}. The quantum component of uncertainty arises when the applied measurement does not commute with the observed quantum system, causing a spread in the measurement outcomes. This quantum-caused uncertainty can be captured, for instance, by skew information³³ and quantum coherence^{34,35} w.r.t. the observable and the quantum state. Spurred by this concept, we propose a novel complementarity relation for a steering witness in this work. Specifically, we reveal a complementarity relation between the quantum part (the distillable coherence) and the classical part (the von-Neumann entropy) of a system's total uncertainty. We prove that this relation is a necessary condition of the EUR. As a direct implication, a quantum-classical uncertainty complementarity relation (QCUR) emerges as a stronger steering witness in terms of detection efficiency. Additionally, we prove that the QCUR-based steering witness can detect all pure entangled states, while the EUR, the complementarity of coherence for mutually unbiased bases, and Reid's criteria cannot. This aspect is also validated by a linear optical experiment as reported here. Furthermore, it is known that quantum steering is closely related to measurement incompatibility. We show that the violation of the QCUR can be used to quantify measurement incompatibility, thereby revealing a deeper connection between the generalized uncertainty principle as well as quantum steering. For completeness, we also investigate other properties of the QCUR-based steering witness. This includes the asymmetric nature, the ability to detect one-way steering, and its monotonic behavior. Our work uncovers a deeper connection between quantum coherence and the uncertainty principle, highlighting its superior utility for steering detection.

Results

Distillable coherence and quantum-classical uncertainty complementarity

In this section, we derive the QCUR from the distillable coherence. To begin with, we provide a concise overview of coherence distillation³⁷. Given a priori reference basis $\{|i\rangle\}_i$, a quantum state ρ is considered incoherent if it is diagonal with respect to the reference basis, i.e., $\rho = \sum_i p_i |i\rangle\langle i|$, where p_i forms a probability distribution. Thus, states that are not in this form are categorized as coherent states³⁸. We denote the set of incoherent states as \mathcal{I} . Furthermore, a quantum operation Λ is identified as a quantum-incoherent operation (QIO) if it maps an arbitrary incoherent state to another incoherent state. For ease of expression, we sometimes extend the term QIOs to refer to the set of quantum incoherent operations.

A coherence distillation process involves the utilization of QIOs to convert n copies of general quantum states into the single-qubit maximally coherent state $|\Phi_2\rangle = \sum_{i=0}^1 |i\rangle / \sqrt{2}$ with a rate R ³⁷. In the asymptotic limit, i.e., $n \rightarrow \infty$, the maximal rate is called the distillable coherence: $C_d(\rho) = \sup \left\{ R : \lim_{n \rightarrow \infty} \inf_{\Lambda \in \text{QIO}} \|\Lambda(\rho^{\otimes n}) - \Phi_2^{\otimes Rn}\| = 0 \right\}$, where $\|\bullet\|$ denotes the trace norm. As reported in Ref.³⁷, the distillable coherence has a closed form:

$$C_d(\rho) = H_\Delta(\rho) - S(\rho), \quad (1)$$

where $S(\rho) = -\text{Tr} \rho \log_2 \rho$ is the von-Neumann entropy. Here, we adopt $H_\Delta(\rho) = S[\Delta(\rho)]$ as a shorthand notation characterizing the Shannon entropy of the state under the reference basis, where $\Delta(\cdot) = \sum_i |i\rangle\langle i| \cdot |i\rangle\langle i|$ represents the complete decoherence operation, e.g. $\Delta(\rho) = \sum_i p_i |i\rangle\langle i|$. Note that a state ρ is distillable (i.e. $C_d > 0$) if and only if $\rho \notin \mathcal{I}$.

To obtain the QCUR, we adopt the notion of "quantum uncertainty" described in Refs.^{33,34,39}. Specifically, it is known that the von-Neumann entropy $S(\rho)$ characterizes the "classical part of uncertainty" as it aligns with the classical notion, where the uncertainty originates from the lack of information of a system and increases under classical mixing. In addition, the Shannon entropy $H_\Delta(\rho)$ captures the "total uncertainty" or the observed uncertainty characterized by the probability distribution $\{p_i\}_i$. Therefore, according to Eq. (1), $C_d(\rho)$ quantifies quantum coherence, i.e. the amount of observed uncertainty that cannot be explained by classical ignorance of the system. Along with this reasoning, the distillable coherence can be interpreted as quantum uncertainty. Through a rearrangement of Eq. (1), i.e., $C_d(\rho) + S(\rho) = H_\Delta(\rho)$, one can obtain the QCUR, where the total uncertainty is constituted by the quantum and classical uncertainties^{33,34,39–43}. An equivalent inequality for the QCUR can be expressed as

$$H_\Delta(\rho) \geq C_d(\rho), \quad (2)$$

which means that quantum uncertainty $C_d(\rho)$ cannot exceed the total uncertainty $H_\Delta(\rho)$. Note that the inequality is saturated when ρ is a pure state, given that there is no classical uncertainty.

Violation of quantum-classical uncertainty complementarity by quantum steering

The QCUR holds for all local quantum states in a similar manner to other uncertainty relations. As aforementioned, it is known that quantum steering can violate the local uncertainty principle. One can therefore expect that steering can also break

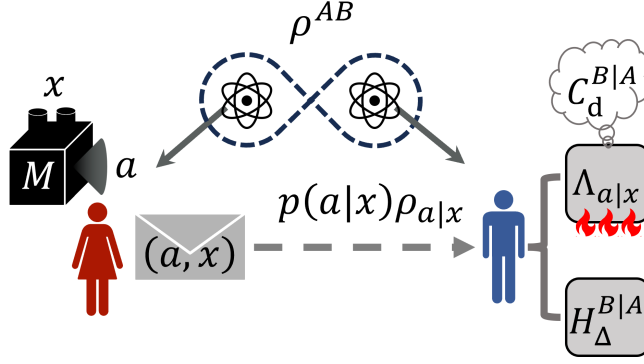


Figure 1. Schematic illustration of the steering-assisted coherence distillation scenario. A bipartite system ρ^{AB} is shared by Alice and Bob. Alice measures her subsystem with a measurement setting x and obtains outcome a with probability $p(a|x)$. After that, she sends the information (a, x) to Bob through classical communication. Depending on the measurement setting, Bob decides whether to perform coherence distillation by $\Lambda_{a|x}$ or to compute the conditional Shannon entropy $H_{\Delta}^{B|A}$ on the conditional state $\rho_{a|x}$.

the QCUR. To formalize this idea, we introduce a steering-assisted coherence distillation task, as described in Fig. 1. Suppose that Alice and Bob share a bipartite state ρ^{AB} . Alice performs a set of positive operator-valued measures (POVM), denoted as $\mathcal{M} = \{M_{a|x}\}_{a,x}$ satisfying $M_{a|x} \geq 0 \forall a, x$ and $\sum_a M_{a|x} = \mathbb{1} \forall x$. Here, x denotes the measurement settings and a represents the corresponding outcomes. The measurement results can be succinctly represented by a conditional probability distribution $p(a|x)$. After the measurements, Alice communicates both the outcome a and the setting x to Bob, where we denote Bob's conditional state as $\rho_{a|x}$. Conventionally, these results can be summarized by a state assemblage defined by $\mathcal{A} = \{\sigma_{a|x}\}_{a,x}$ with $\sigma_{a|x} = p(a|x)\rho_{a|x} \forall a, x$.

It is known that one can employ the local-hidden-state (LHS) model to determine whether a given assemblage is steerable or not. Specifically, an assemblage \mathcal{A}^{LHS} admits an LHS model when its elements can be described by¹:

$$\sigma_{a|x}^{\text{LHS}} = \sum_{\lambda} p(\lambda) p(a|x, \lambda) \rho_{\lambda} \quad \forall a, x, \quad (3)$$

where $\{\rho_{\lambda}\}_{\lambda}$ and $\{p(a|x, \lambda)\}_{a,x}$ are, respectively, the hidden states and probabilities that constitute a stochastic process mapping the hidden variable λ into the observable outcomes $a|x$. For convenience, we also consider the state assemblage for a fixed setting x , denoted as $\mathcal{A}_x = \{\sigma_{a|x}\}_a$. Based on the Alice measurement setting, Bob can either distill the quantum coherence or perform projective measurements with the reference bases to obtain the Shannon entropy. Note that with the help of Alice's classical communication, Bob can adjust the local incoherent operation $\Lambda_{a|x}$ to optimize his distillable coherence. We can then obtain the conditional distillable coherence and the Shannon entropy for a given setting x , which are respectively defined as

$$\begin{aligned} C_d^{B|A}(\mathcal{A}_x) &= \sum_a p(a|x) C_d(\rho_{a|x}), \\ H_{\Delta}^{B|A}(\mathcal{A}_x) &= \sum_a p(a|x) H_{\Delta}(\rho_{a|x}). \end{aligned} \quad (4)$$

By utilizing the convexity of C_d , we show that the conditional distillable coherence can be upper-bounded for all LHS models, namely, $C_d^{B|A}(\mathcal{A}_x^{\text{LHS}}) \leq \sum_{\lambda} p(\lambda) H_{\Delta}(\rho_{\lambda})$. Likewise, the conditional Shannon entropy possesses a lower bound by its concavity, namely $H_{\Delta}^{B|A}(\mathcal{A}_x^{\text{LHS}}) \geq \sum_{\lambda} p(\lambda) H_{\Delta}(\rho_{\lambda})$. We can then derive the QCUR-based steering inequality:

$$H_{\Delta}^{B|A}(\mathcal{A}_{x'}^{\text{LHS}}) \geq C_d^{B|A}(\mathcal{A}_x^{\text{LHS}}) \quad \forall x, x'. \quad (5)$$

Consequently, *quantum steerability can be captured as the violation of the QCUR*. Hereafter, we use the optimal violation of the complementary relation of uncertainty to quantify the generalized uncertainty relation induced by Alice's measurement, in terms of measurement incompatibility.

Quantum-classical uncertainty complementarity as a necessary condition for the EUR

Upon initial examination, the proposed QCUR and conventional notion of the uncertainty principle appear notably distinct. While the former depends on decomposing the uncertainty into classical and quantum components, the latter emphasizes

the uncertainty trade-off between incompatible variables or bases. Nevertheless, we uncover the interesting connections between these two concepts. Specifically, we prove that the QCUR is a necessary condition for the EUR, which captures the unpredictability of the results from two observables^{21,22}. From the aspect of a steering witness, the QCUR is stronger than the EUR in terms of the detection efficiency. In the next section, we further prove that the QCUR-based steering criterion can detect all pure entangled states, while the other criteria cannot.

Recall that the EUR and the EUR-based steering inequality for a pair of non-commuting projective measurements are, respectively, expressed as:

$$H_{\Delta}(\rho) + H_{\Delta'}(\rho) \geq -\log \Omega, \quad (6)$$

and $H_{\Delta}^{B|A}(\mathcal{A}_x^{\text{LHS}}) + H_{\Delta'}^{B|A}(\mathcal{A}_{x'}^{\text{LHS}}) \geq -\log \Omega.$

Here, to keep the notation consistent, we encode the bases for these two measurements ($\{|i\rangle\}_i$ and $\{|j\rangle\}_j$) into the pure dephasing maps (Δ and Δ') such that $H_{\Delta}(\rho) = \sum_i \langle i|\rho|i\rangle \log \langle i|\rho|i\rangle$ and $H_{\Delta'}(\rho) = \sum_j \langle j|\rho|j\rangle \log \langle j|\rho|j\rangle$. In addition, $\Omega = \max_{i,j} |\langle i|j\rangle|^2$ denotes the maximal overlap between the two measurement bases. The interpretation of this EUR-based steering criterion is that after Alice obtains her measurement data, if she can predict Bob's measurement result with the uncertainty lower than the EUR allows, then Bob's local quantum states which can reproduce such results do not exist.

By utilizing the contraction property of the relative entropy and the monotonicity of the logarithm function (see "Methods" for the detailed derivations), one can show that

$$H_{\Delta}(\rho) \geq C_d(\rho) \geq -H_{\Delta'}(\rho) - \log \Omega. \quad (7)$$

Therefore, the QCUR emerges as a necessary condition for the EUR. Following a similar procedure, one can further deduce that the QCUR-based steering inequality is stronger than the EUR-based steering inequality. Specifically, a state assemblage that violates the QCUR-based steering inequality also violates the EUR-based steering inequality but not *vice versa*.

Properties of the QCUR-based steering inequality violation

Based on Eq. (5), now we define the steering inequality violation parameter (SIVP) as

$$\mathcal{V}_S(\mathcal{A}) := \max \left\{ \max_x C_d^{B|A}(\mathcal{A}_x) - \min_x H_{\Delta}^{B|A}(\mathcal{A}_x), 0 \right\}, \quad (8)$$

where $\max\{x_1, x_2\} = x_1$, if $x_1 > x_2$; $\max\{x_1, x_2\} = x_2$ otherwise. By this definition, the SIVP vanishes if a given state assemblage admits an LHS model. Furthermore, we show that the SIVP satisfies the following properties, and the proofs can be found in "Methods."

Property 1. The SIVP is asymmetric. In the sense that the values of the SIVP are different for Alice to Bob and vice versa.

A steering test should be naturally asymmetrical, and this distinction becomes evident as discussed in previous works^{16,44,45}, that permits steering to occur in a unidirectional manner; specifically, from Alice to Bob.

With this property in hand, we can directly show the following.

Property 2. The SIVP can detect one-way steering.

In the steering scenario, Alice and Bob each have distinct roles. Therefore, the presence of steerability in one direction (e.g., from Alice to Bob) does not guarantee its existence in the opposite direction (from Bob to Alice)^{44,45}. Several examples are provided in "Methods."

Property 3. The SIVP can detect all pure entangled states.

It is known that all pure entangled states are steerable^{1,46}. More specifically, we show that for all pure bipartite entangled states $|\psi\rangle^{AB} = \sum_i \sqrt{p_i} |i\rangle \otimes |i\rangle$, there exists a set of Alice's measurement and a reference basis $\{|i\rangle\}_i$ such that $\mathcal{V}_S > 0$ (see "Methods" for details). This property showcases that the SIVP is also a witness of entanglement when evaluated on pure entangled states and is distinct from other coherence-based steering inequalities²⁴. Later, we also show the experimental demonstration of the SIVP for pure entangled states. Note that this property highlights the efficiency of the QCUR-based SIVP for detecting steerability, given that other criteria (e.g. the EUR, complementarity of coherence for mutually unbiased, and Reid's criteria) cannot reveal this property.

One can ask whether the SIVP can serve as a steering monotone^{47,48}. In the most general setting under the resource theory of quantum steering⁴⁹, the answer is negative, because the SIVP does not monotonically decrease under one-way local operations and classical communications (see "Methods" for details). However, the SIVP could be non-increasing if we restrict the local operations to be QIOs^{37,38,50}, as suggested by the numerical results included in "Methods". Now, we prove that the SIVP is a non-increasing function under genuine incoherent operations (GIOs), which form a subset of the QIOs⁵¹.

Property 4. The SIVP is a convex-non-increasing function under genuine incoherent operations.

The main idea of the proof is based on the diagonalization of a GIO w.r.t. the reference basis. According to Ref.⁵¹, there must exist a Kraus representation of the GIO, such that all Kraus operators of the GIO are diagonalized w.r.t. the reference basis. Using this property, one can show that the distillable coherence (the Shannon entropy) monotonically decreases (increases) under the GIO, implying that \mathcal{V}_S also monotonically decreases under the GIO. With this property, one can further show that the SIVP is non-increasing under one-way local GIOs and classical communications.

We also emphasize the restriction of GIOs on the local operation in our study makes sense given the fact that the SIVP is based on the distillable coherence. If we allow the most general local operations, the coherence can be distilled by merely changing the local reference basis (see also the discussion in Refs.^{50,52-55}). In this sense, the general local operation makes a false violation of the SIVP (see also numerical evidence in the ‘‘Methods’’). With this property, we can show that the SIVP can be used to quantify measurement incompatibility⁵⁶⁻⁵⁸.

Quantifying measurement incompatibility

We start by introducing the incompatible measurements. If multiple physical observables cannot be measured simultaneously, we call these measurements incompatible. It is a fundamental characteristic arising from various quantum phenomena, e.g., Bell inequality violation^{59,60}, Kochen-Specker contextuality⁶¹, and uncertainty principles (c.f., section ‘‘Distillable coherence and quantum-classical uncertainty complementarity’’)^{38,62,63}. Given a set of POVMs $\mathcal{M} = \{M_{a|x}\}_{a,x}$, it is compatible (or jointly measurable) if it can be expressed by

$$M_{a|x} = \sum_{\lambda} p(a|x, \lambda) G_{\lambda}, \quad (9)$$

where $\{G_{\lambda}\}_{\lambda}$ is a parent POVM and $p(a|x, \lambda)$ is a conditional probability. One can observe that the joint measurable model and the LHS model in Eq. (3) are a mathematically similar. Given a state assemblage, it can be transmitted to a set of POVMs via the concept of the steering-equivalent observables (SEO) $\mathcal{B} = \{B_{a|x}\}_{a,x}$, i.e., $B_{a|x} = (\rho_B)^{-1/2} \sigma_{a|x} (\rho_B)^{-1/2}$, with $\rho_B = \sum_a \sigma_{a|x}$ ²⁶⁻²⁸. We note that once ρ_B was not full rank, the same expression can be obtained by considering an additional isometry (see also Ref.²⁸). One can observe that the SEO is incompatible if and only if the state assemblage is steerable²⁸.

Inspired by the very recently proposed steering-induced incompatible measure⁶⁴, we are able to quantify measurement incompatibility by the steering-assisted coherence distillation, namely

$$\mathcal{V}_1(\mathcal{B}) = \sup_{\rho_B} \mathcal{V}_S[\sqrt{\rho_B} \mathcal{B} \sqrt{\rho_B}], \quad (10)$$

where sup is taking over all full-rank states ρ_B , and \mathcal{V}_S is the SIVP defined in Eq. (8). We then can show the following:

Property 5. The optimal steering-assisted coherence distillation $\mathcal{V}_1(\mathcal{B})$ is a valid incompatibility monotone⁵⁶ in the sense that it satisfies: (a) $\mathcal{V}_1(\mathcal{B}) = 0$ if \mathcal{B} is jointly measurable; (b) $\mathcal{V}_1(\mathcal{B})$ satisfies convexity; (c) $\mathcal{V}_1(\mathcal{B})$ is non-increasing under post-processing, namely

$$\{B_{a'|x'}\}_{a',x'} = \mathcal{W}(\{B_{a|x}\}_{a,x}) = \sum_{a,x} p(x|x') p(a'|a,x,x') \{B_{a|x}\}_{a,x}, \quad (11)$$

where $p(x|x')$ and $p(a'|a,x,x')$ are the conditional probabilities and \mathcal{W} is a post-processing scenario defined as a deterministic wiring map⁴⁹.

This result further strengthens the application of the steering-assisted coherence distillation (see ‘‘Methods’’ for details). In one direction, it quantitatively connects measurement incompatibility with quantum coherence and gives an additional concrete example for a steering-induced incompatible measure⁶⁵. In the other direction, we clearly provide a different operational interpretation of measurement incompatibility. Specifically, if we consider ρ^{AB} is a pure entangled state, the SEO \mathcal{B} of \mathcal{A} generated by \mathcal{M} is exactly equivalent to \mathcal{M} . In this sense, the measurement incompatibility of \mathcal{M} can be accessed in a steering-assisted coherence distillation by properly choosing the pure state ρ^{AB} , such that $\mathcal{V}_1(\mathcal{M}) = \sup_{\rho_B} \mathcal{V}_S[\sqrt{\rho_B} \mathcal{M} \sqrt{\rho_B}]$.

Experimental demonstration

To support the derived theoretical framework, we have performed experimental testing on the platform of linear optics encoding two-qubit states into polarizations of photon pairs. The experimental setup, as depicted in Fig. 2a, consists of a laser emitting pulses at 355 nm that impinge into a crystal cascade made of two β -BaB₂O₄ crystals (2×BBO). These crystals are 1 mm thick and are mutually positioned, so that their optical axes lie in mutually perpendicular planes⁶⁶. In these crystals, the laser beam is subjected to the nonlinear process of type-I spontaneous parametric down-conversion. In the first crystal, horizontally polarized laser photons are converted into pairs of vertically polarized photons at 710 nm. The second crystal

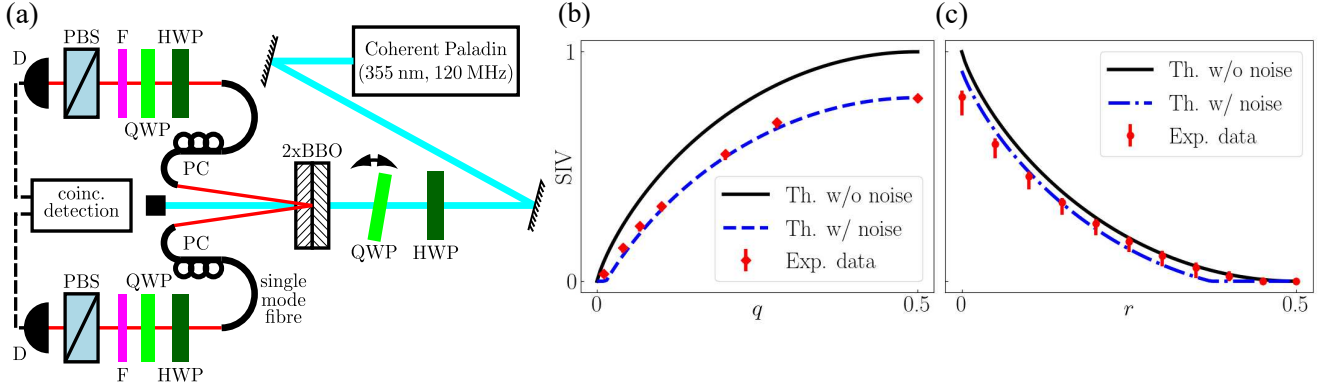


Figure 2. (a) Schematic of the experimental setup. Individual components are labelled as follows: BBO: β -BaB₂O₄ crystal, HWP: half-wave plate, QWP: quarter-wave plate, F: interference bandpass filter (5 nm spectral width), PBS: polarizer, PC: fiber polarization controller, D: single-photon avalanche photodiode. (b) The theoretical predictions are juxtaposed with the experimental results of pure entangled states. The black solid curve shows the noise-free theoretical outcomes given by $SIVP(q) = H_b(q)$, which is the binary entropy of the parameter q . Meanwhile, the blue-dashed curve represents the theoretical predictions incorporating the optimal white noise factor $p_0 = 0.026$; the red diamonds indicate experimental results, with error bars obtained via the Monte Carlo method as described in the text. (c) The theoretical predictions are compared with the experimental results of the Bell diagonal state. The black solid curve shows the noise-free theoretical outcomes given by $SIVP(r) = 1 - H_b(r)$; the blue-dashed-dotted curve represents the theoretical predictions incorporating the noise factors $p_+ = 0.009$ and $p_- = 0.013$ respectively; the red bullets showcase the experimental results.

facilitates the creation of horizontally-polarized photon pairs from the vertically polarized laser beam. Photon pairs generated in both crystals are subsequently collected into single-mode optical fibers. Coherence of the laser beam and indistinguishability in the photons collection assure the effective generation of the photon pairs in a superposition state of both contributing processes, $|\Phi(q, \phi)\rangle = \sqrt{q}|HH\rangle + e^{i\phi}\sqrt{1-q}|VV\rangle$, where H and V stand for the horizontal and vertical polarization states, respectively. The parameters q and ϕ are controlled by tuning the laser-beam polarization using half- and quarter-wave plates.

The aforementioned single-mode fibers guide the photon pairs to the state detection and the analysis part of the setup. A series of half- and quarter-wave plates followed by a polarizer implement local projections onto any pure polarization state. Such polarization projection is implemented independently on both photons of a pair. We project the photon pairs onto all the combinations of the eigenstates of the Pauli matrices and register the number of simultaneous two-photon detections for all these combinations⁶⁷. A method of maximum likelihood is then used to estimate the most probable density matrix fitting the registered counts⁶⁸. This density matrix is then used to calculate the corresponding SIVP.

To evaluate the experimental uncertainty of the calculated SIVP, we use the fact that registered photon detections follow the Poisson statistics (shot-noise). A Monte-Carlo method is implemented, where all registered counts are randomized assuming the Poisson statistics with the mean value being the actual experimentally observed value. Subsequently the maximum-likelihood method is deployed to estimate the density matrix, which is then used to calculate the SIVP. By repeating this procedure 1000 times, we obtain the statistics of the SIVP under the detection shot-noise and establish the confidence intervals, $\pm\sigma$.

Any experimental implementation is, at least to some degree, imperfect. Partial distinguishability in the generating crystal and imperfections of polarization optics lead to a non-unit purity of the generated states. These imperfections can be reasonably well modeled by white noise. To estimate the amount of such noise, we maximize the expression $F(\rho_{p_0}, \rho_{\text{exp}}) = \max_p (\text{Tr} \sqrt{\sqrt{\rho_p} \rho_{\text{exp}} \sqrt{\rho_p}})^2$, where F denotes the Bures fidelity, ρ_{exp} is the experimentally observed density matrix and $\rho_p = (1-p)\rho_{\text{th}} + p\mathbb{1}/4$ is the theoretical density matrix ρ_{th} with added white noise. We have found that for the series of the noisy quasi-pure states ρ_p and presented in Fig. 2b, the optimal value of the white-noise factor p is $p_0 = 0.026$ on average.

In Fig. 2b, we compare the theoretical predictions with the experimental results. The noise-free theoretical predictions, i.e., $SIVP(q) = H_b(q)$, where $H_b(x) = -x \log_2 x - (1-x) \log_2 (1-x)$ is the binary entropy, are represented as the black solid curve. Note that due to the convexity of quantum states, the maximization of Eq. (10) occurs when Alice and Bob share a pure entangled state. In our experimental setup, therefore, the measurement incompatibility \mathcal{I}_1 can be quantified in terms of steering-assisted coherence distillation when $q = 0.5$ [cf., Eq. (10)]. The predictions with a noise factor $p_0 = 0.026$ are shown with blue-dashed curves. The experimental results are shown in red diamonds with error bars obtained via the above mentioned Monte Carlo method.

Additionally, we present the results for Bell diagonal states in Fig. 2c, obtained through numerical interpolation between

two experimentally maximized entangled and mutually orthogonal Bell states: $|\Phi^+\rangle = |\Phi(1/2, 0)\rangle$ and $|\Phi^-\rangle = |\Phi(1/2, \pi)\rangle$. A Bell diagonal state is defined as $\rho_{\text{Bell}} = r|\Phi^+\rangle\langle\Phi^+| + (1-r)|\Phi^-\rangle\langle\Phi^-|$. The noise-free theoretical predictions are expressed as $\text{SIVP}(r) = 1 - H_b(r)$, depicted by the black solid curve. The experimental setup was meticulously calibrated to generate the purest states possible, reducing noise to $p_+ = 0.009$ and $p_- = 0.013$, represented by the blue-dashed-dotted curve. Finally, our experimental results for the Bell diagonal states are shown as red bullets with error bars.

Discussion

In this work, we proposed a novel complementarity relation, termed QCUR for steering detection. We prove that the QCUR is a necessary condition for the EUR. Consequently, the QCUR emerges as the most efficient steering witness compared with the EUR, the complementarity of coherence for mutually unbiased bases, and Reid's criteria. Further, we showed that the QCUR-based steering witness can detect all pure entangled states. A linear optical experiment was also performed to validate this result. Furthermore, we showed that violation of the QCUR can be used to quantify measurement incompatibility. In addition, we showed that the QCUR-based steering witness is asymmetric, capable of detecting one-way steering, and is monotonic under GIOs.

Future works include extending the proposed scenario to one-shot^{52,69} and asymptotic reversibility settings⁷⁰. In addition, it raises an intriguing open question: can these distillation scenarios also detect and possibly quantify quantum steering?

Methods

Derivation of the QCUR-based steering inequality

For convenience, we define the optimal conditional distillable coherence and the conditional Shannon entropy as

$$C_d^*(\mathcal{A}) := \max_x C_d^{B|A}(\mathcal{A}_x) \quad \text{and} \quad H_\Delta^*(\mathcal{A}) := \min_x H_\Delta^{B|A}(\mathcal{A}_x), \quad (12)$$

respectively.

Proof. —The inequality $C_d^*(\mathcal{A}) \leq H_\Delta^*(\mathcal{A})$ holds if the assemblage \mathcal{A} admits an LHS model.

Considering that the assemblage received by Bob can be described by the LHS model, the upper bound of the coherence distillation can be readily obtained:

$$\begin{aligned} C_d^*(\mathcal{A}) &= \max_x \sum_a p(a|x) C_d \left[\sum_\lambda p(\lambda|a,x) \rho_\lambda \right] \\ &= \max_x \sum_a p(a|x) C_d \left[\sum_\lambda \frac{p(a|x, \lambda) p(\lambda)}{p(a|x)} \rho_\lambda \right] \\ &\leq \max_x \sum_a p(a|x) \sum_\lambda \frac{p(a|x, \lambda) p(\lambda)}{p(a|x)} C_d(\rho_\lambda) \\ &= \max_x \sum_\lambda p(\lambda) C_d(\rho_\lambda) \\ &= \sum_\lambda p(\lambda) C_d(\rho_\lambda) \\ &\leq \sum_\lambda p(\lambda) H_\Delta(\rho_\lambda). \end{aligned} \quad (13)$$

Since $H_\Delta(\rho)$ is concave in ρ , we readily obtain $\sum_\lambda p(\lambda) H_\Delta(\rho_\lambda) \leq H_\Delta^*(\mathcal{A})$ by an analogous derivation. This concludes the proof of steering inequality:

$$C_d^*(\mathcal{A}) \leq H_\Delta^*(\mathcal{A}) \quad \text{if } \mathcal{A} \in \text{LHS}. \quad (14)$$

□

Proof for the QCUR as a necessary condition for the EUR

We first compare the QCUR and EUR, showing that one can relax the lower bound of the QCUR to obtain the EUR, that is

$$\begin{aligned}
H_{\Delta}(\rho) &\geq C_d(\rho) \\
&= D[\rho||\Delta(\rho)] \\
&\geq D[\Delta(\rho)||\Delta' \circ \Delta(\rho)] \\
&= \text{Tr } \Delta'(\rho) \log [\Delta'(\rho) - \Delta' \circ \Delta(\rho)] \\
&= -H_{\Delta'}(\rho) - \sum_j \langle j|' \rho |j\rangle' \log \sum_i |\langle i|j\rangle'|^2 \langle i| \rho_{a|x'} |i\rangle \\
&\geq -H_{\Delta'}(\rho) - \sum_j \langle j|' \rho |j\rangle' \log \left(\max_{i,j} |\langle i|j\rangle'|^2 \right) \sum_i \langle i| \rho_{a|x'} |i\rangle \\
&= -H_{\Delta'}(\rho) - \log \Omega,
\end{aligned} \tag{15}$$

where $D(\rho||\sigma) = \text{Tr } \rho (\log \rho - \log \sigma)$ is the relative entropy, $\Delta'(\rho) = \sum_j \langle j|' \rho |j\rangle' |j\rangle' \langle j|'$ is an arbitrary complete decoherence operation in the basis $\{|j\rangle'\}_j$, and $\Omega = \max_{i,j} |\langle i|j\rangle'|^2$ represents the maximal overlap between two different reference bases. Note that the second inequality is given by the contraction of the relative entropy²² and the third inequality is due to the applied maximization. The result indicates that satisfying the QCUR is a necessary condition of the EUR.

Next, we show that the QCUR-based steering inequality is stronger than the EUR-based steering inequality²². We start from the steering inequality in Eq. (5) by taking two Alice's measurement settings x and x' , we have

$$\begin{aligned}
\sum_a p(a|x) H_{\Delta}(\rho_{a|x}) &\geq \sum_a p(a|x') C_d(\rho_{a|x'}) \quad \forall x, x' \\
&= \sum_a p(a|x') \{ D[\rho_{a|x'} || \Delta(\rho_{a|x'})] \} \\
&\geq \sum_a p(a|x') \{ D[\Delta'(\rho_{a|x'}) || \Delta' \circ \Delta(\rho_{a|x'})] \} \\
&= \sum_a p(a|x') \text{Tr } \Delta'(\rho_{a|x'}) [\log \Delta'(\rho_{a|x'}) - \log \Delta' \circ \Delta(\rho_{a|x'})] \\
&= -\sum_a p(a|x') H_{\Delta'}(\rho_{a|x'}) - \sum_a p(a|x') \sum_j \langle j|' \rho_{a|x'} |j\rangle' \log \sum_i |\langle i|j\rangle'|^2 \langle i| \rho_{a|x'} |i\rangle \\
&\geq -\sum_a p(a|x') H_{\Delta'}(\rho_{a|x'}) - \log \Omega.
\end{aligned} \tag{16}$$

The above result directly implies the EUR for unsteerable states²², i.e.,

$$\sum_a p(a|x) H_{\Delta}(\rho_{a|x}) + \sum_a p(a|x') H_{\Delta'}(\rho_{a|x'}) \geq -\log \Omega. \tag{17}$$

Therefore, we conclude that the QCUR-based inequality in Eq. (5) is a stronger criterion compared to the EUR-based one.

For completeness, we provide a detail derivation from the conventional conditional Shannon entropy $H(\mathbb{B}|\mathbb{A})$, applying the notation used in this paper, i.e., $H_{\Delta}^{B|A}$. Consider the product measurements $\mathbb{A} \otimes \mathbb{B}$ for two projective measurements $\mathbb{A} = \{|\mathbb{A}_a\rangle \langle \mathbb{A}_a|\}_a$ and $\mathbb{B} = \{|\mathbb{B}_b\rangle \langle \mathbb{B}_b|\}_b$ performed by Alice and Bob on their own systems, the joint distribution $p(a, b)$ and the conditional Shannon entropy $H(\mathbb{B}|\mathbb{A})$ read:

$$\begin{aligned}
H(\mathbb{B}|\mathbb{A}) &= H(\mathbb{A}, \mathbb{B}) - H(\mathbb{A}) \\
&= \sum_{a,b} p(a, b|\mathbb{A}, \mathbb{B}) \log p(a, b|\mathbb{A}, \mathbb{B}) - \sum_a p(a|\mathbb{A}) \log p(a|\mathbb{A}) \\
&= \sum_{a,b} p(a|\mathbb{A}) p(b|a, \mathbb{A}, \mathbb{B}) [\log p(b|a, \mathbb{A}, \mathbb{B}) + \log p(a|\mathbb{A})] - \sum_a p(a|\mathbb{A}) \log p(a|\mathbb{A}) \\
&= \sum_{a,b} p(a|\mathbb{A}) p(b|a, \mathbb{A}, \mathbb{B}) \log p(b|a, \mathbb{A}, \mathbb{B}) \\
&= \sum_a p(a|\mathbb{A}) \sum_b \langle \mathbb{B}_b | \rho_{a|\mathbb{A}} | \mathbb{B}_b \rangle \log \langle \mathbb{B}_b | \rho_{a|\mathbb{A}} | \mathbb{B}_b \rangle,
\end{aligned} \tag{18}$$

where we can find that $H(\mathbb{B}|\mathbb{A})$ is equivalent to $H_{\Delta}^{B|A}$ by choosing $\Delta(\rho) = \sum_b \langle \mathbb{B}_b | \rho | \mathbb{B}_b \rangle$.

Proof of Property 1: Asymmetry of the steering inequality violation

Proof. —To demonstrate the asymmetry, we consider general two-qubit states defined by

$$\chi(\vec{r}, \vec{s}, \vec{t}) = \frac{1}{4} \left(\mathbb{1} \otimes \mathbb{1} + \vec{r} \cdot \vec{\sigma} \otimes \mathbb{1} + \mathbb{1} \otimes \vec{s} \cdot \vec{\sigma} + \sum_{i,j=1}^3 t_{ij} \sigma_i \otimes \sigma_j \right), \quad (19)$$

where $\{\vec{r}, \vec{s}, \vec{t}\}$ are the vectors with norm less than unit and $\vec{\sigma} = (\sigma_1, \sigma_2, \sigma_3)$ is the Pauli vector. If the SIVP is asymmetric, the value of the SIVP depends on the local Bloch vector, i.e., \vec{r} and \vec{s} . Here, we consider Alice performing measurements described by $M_{a|x} = [\mathbb{1} + (-1)^a \sigma_x]/2$, with $a \in \{0, 1\}$ and $x \in \{1, 3\}$; where σ_1 and σ_3 are the Pauli X and Z matrices, respectively, then the assemblage received by Bob becomes

$$\begin{aligned} \sigma_{a|x} &= \text{Tr}_A [M_{a|x} \otimes \mathbb{1} \chi(\vec{r}, \vec{s}, \vec{t})] \\ &= \frac{1}{4} \text{Tr}_A \left[M_{a|x} \otimes \mathbb{1} + M_{a|x} \vec{r} \cdot \vec{\sigma} \otimes \mathbb{1} + M_{a|x} \otimes \vec{s} \cdot \vec{\sigma} + \sum_{i,j=0}^2 M_{a|x} t_{ij} \sigma_i \otimes \sigma_j \right] \\ &= \frac{1}{4} \left\{ \mathbb{1} + \frac{1}{2} \text{Tr}[\vec{r} \cdot \vec{\sigma} + (-1)^a \sigma_x \vec{r} \cdot \vec{\sigma}] \mathbb{1} + \vec{s} \cdot \vec{\sigma} + \frac{1}{2} \sum_{i,j=0}^2 t_{ij} \text{Tr}[\sigma_i + (-1)^a \sigma_x \sigma_i] \sigma_j \right\} \\ &= \frac{1}{4} \left[\mathbb{1} + (-1)^a r_x \mathbb{1} + \vec{s} \cdot \vec{\sigma} + \sum_j (-1)^a t_{xj} \sigma_j \right] \\ &= \frac{1}{2} \left[1 + (-1)^a r_x \right] \times \frac{1}{2} \left[\mathbb{1} + \sum_j \frac{s_j + (-1)^a t_{xj}}{1 + (-1)^a r_x} \sigma_j \right], \end{aligned} \quad (20)$$

with probability $\text{Tr} \sigma_{a|x} = [1 + (-1)^a r_x]/2$. To obtain the SIVP, we need to calculate the eigenvalue of the reduced state $\rho_{a|x}$ and its dephased counterpart $\Delta(\rho_{a|x}) = \sum_{i=0}^1 \langle i | \rho_{a|x} | i \rangle | i \rangle \langle i |$, which are, respectively,

$$E_{a|x,\pm}(r, s, t) = \frac{1}{2} \left[1 \pm \frac{\sqrt{\sum_j [s_j + (-1)^a t_{xj}]^2}}{1 + (-1)^a r_x} \right] \quad \text{and} \quad E_{a|x,\pm}^{\text{deph}}(r, s, t) = \frac{1}{2} \left[1 \pm \frac{s_0 + (-1)^a t_{x,0}}{1 + (-1)^a r_x} \right]. \quad (21)$$

Here, we can observe that the SIVP in Eq. (12) depends on the local Bloch vectors \vec{r} and \vec{s} . As we swap the general two-qubit states $\text{SWAP}[\chi(\vec{r}, \vec{s}, \vec{t})] = \chi(\vec{s}, \vec{r}, \vec{t})$, we obtain different values of SIVP, which states that the SIVP is asymmetric. \square

Example of Property 2: Detecting one-way steering

As a concrete example, we now present the SIVP of a set of states described by

$$\chi(s, q) = s |\psi_q\rangle \langle \psi_q| + (1-s) \text{Tr}_B(|\psi_q\rangle \langle \psi_q|) \otimes \mathbb{1}/2, \quad (22)$$

where $|\psi_q\rangle = \sum_{i=0}^1 t_i(q) |i\rangle \otimes |i\rangle$, $t_0(q) = q$, and $t_1(q) = 1 - q$ in the parameter windows: $s \in [0.75, 1]$ and $q \in [0.001, 0.5]$. The SIVP values are shown in Fig. 3. In the light-red area (I), the steerability can be detected from both directions, i.e., $\mathcal{V}_S(\mathcal{A}^{B \rightarrow A}) > 0$ and $\mathcal{V}_S(\mathcal{A}^{A \rightarrow B}) > 0$. However, in the light-blue area (II), one finds $\mathcal{V}_S(\mathcal{A}^{B \rightarrow A}) = 0$, while $\mathcal{V}_S(\mathcal{A}^{A \rightarrow B}) > 0$, which indicates that the SIVP is only witnessed from Bob to Alice. Finally, in the grey area (III), the steerability cannot be detected from any direction.

Proof of Property 3: Detecting all pure entangled states

For all pure bipartite entangled states, there exists a set of Alice's measurements and a reference basis such that $\text{SIVP} > 0$.

Proof. —Let us consider a set of projective measurements $\{\Pi_{a|x}\}_{a,x}$ for $a, x \in \{0, 1\}$, with one of which (labeled as $x = 0$) satisfying

$$\Pi_{a|x=0} |i\rangle = \delta_{ia} |i\rangle. \quad (23)$$

This specific measurement $\Pi_{a|x=0}$ on Alice's system transforms the conditional state

$$|\psi\rangle_{a|x=0} = \frac{\text{Tr}_A \Pi_{a|x=0} \otimes \mathbb{1} |\psi\rangle^{AB}}{\text{Tr} \Pi_{a|x=0} \otimes \mathbb{1} |\psi\rangle^{AB}} \quad (24)$$

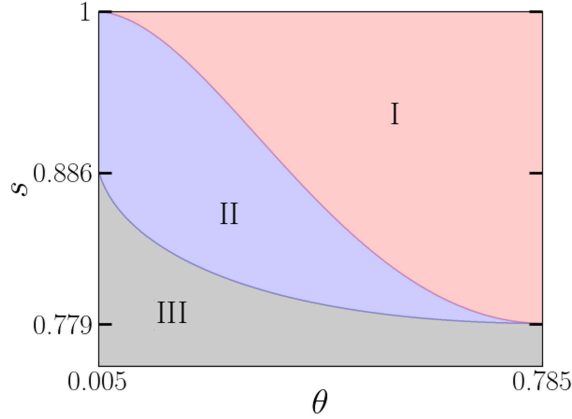


Figure 3. Ability of the steering inequality violation to demonstrate one-way quantum steering in the parameter windows: $s \in [0.75, 1]$ and $q \in [0.001, 0.5]$ for the states in Eq. (22). The light-red area (I) represents both $\mathcal{V}_S(\mathcal{A}^{B \rightarrow A}) > 0$ and $\mathcal{V}_S(\mathcal{A}^{A \rightarrow B}) > 0$, suggesting that quantum steering occurs in both directions. The light-blue area (II), conversely, represents $\mathcal{V}_S(\mathcal{A}^{B \rightarrow A}) > 0$ and $\mathcal{V}_S(\mathcal{A}^{A \rightarrow B}) = 0$, indicating that the respective steerable state only allows Bob to steer Alice. Finally, the grey area (III) represents the range of the parameters s, q such that $\mathcal{V}_S(\mathcal{A}^{B \rightarrow A}) = 0$ and $\mathcal{V}_S(\mathcal{A}^{A \rightarrow B}) = 0$.

into pure and incoherent states. Given that all the conditional states $|\psi\rangle_{a|x}$ remain pure, we have

$$C_d^*(\mathcal{A}) = \max_x \sum_a p(a|x) H_\Delta(|\psi\rangle_{a|x}),$$

$$\text{and } H_\Delta^*(\mathcal{A}) = \min_x \sum_a p(a|x) H_\Delta(|\psi\rangle_{a|x}) = 0,$$
(25)

in which $H_\Delta^*(\mathcal{A}) = 0$ is due to the fact that for all pure states $|\psi\rangle$, $H_\Delta(|\psi\rangle) = 0$ if and only if $\Delta(|\psi\rangle) = |\psi\rangle$. By setting another projective measurement $\{\Pi_{a|x=1}\}_a$, which does not commute with $\{\Pi_{a|x=0}\}_a$, i.e., $[\sum_a a \Pi_{a|x=0}, \sum_{a'} a' \Pi_{a'|x=1}] \neq 0$, we can ensure $C_d^*(\mathcal{A}) > 0$ and, therefore, conclude that $\mathcal{V}_S > 0$. \square

Monotonicity under genuine incoherent operations

Quantum steering has been articulated within the resource theory framework⁴⁹. A measure \mathcal{S} qualifies as a convex steering monotone if it adheres to the following properties:

- (i) $\mathcal{S}(\sigma_{a|x}) = 0$ for all $\sigma_{a|x} \in \text{LHS}$.
- (ii) $\mathcal{S} \left[p\sigma_{a|x} + (1-p)\sigma'_{a|x} \right] \leq p\mathcal{S}(\sigma_{a|x}) + (1-p)\mathcal{S}(\sigma'_{a|x})$, for any real number $0 \leq p \leq 1$ and assemblages $\sigma_{a|x}$ and $\sigma'_{a|x}$.
- (iii) Non-increasing under one-way local operations and classical communication:

$$\sum_\xi p(\xi) \mathcal{S} \left[\frac{\Xi_\xi(\sigma_{a|x})}{\text{Tr} \Xi_\xi(\sigma_{a|x})} \right] \leq \mathcal{S}(\sigma_{a|x}) \quad \forall \sigma_{a|x},$$
(26)

where $p(\xi) = \text{Tr} \Xi_\xi(\sigma_{a|x})$ and $\sum_\xi p(\xi) = 1$.

It is clear that \mathcal{V}_S satisfies properties (i) and (ii). Nonetheless, property (iii) is satisfied only under limited local operations. Property (iii) states that quantum steering should not increase under free operations, e.g., one-way local operations and classical communication⁴⁹.

In the scenario of steering-assisted coherence distillation, local operations must also adhere to incoherent operations. In the following, we consider that these local operations belong to the set of genuine incoherent operations⁵¹, which reside as a subset within incoherent operations⁵⁰.

As shown in Fig. 4, a local stochastic genuine incoherent operation is performed on Bob's system. Specifically, Bob introduces a device that generates a random outcome ξ with probability $p(\xi)$. After receiving the outcome, Bob sends his system into a corresponding genuinely incoherent operation Ξ_ξ ⁵¹, which can be characterized by the set of Kraus operators $\{K_{k,\xi}\}_k$, such that

$$\Xi_\xi(\bullet) = \sum_k K_{k,\xi} \bullet K_{k,\xi}^\dagger \quad \text{with} \quad \sum_k K_{k,\xi}^\dagger K_{k,\xi} = \mathbb{1} \quad \text{and} \quad K_{k,\xi} = \sum_i c_i^{k,\xi} |i\rangle \langle i|.$$
(27)

Additionally, the outcome ξ is also sent to Alice through classical communication, so that she utilizes classical stochastic maps defined by $\{p(a'|a, x, x', \xi), p(x|x', \xi)\}$ to post-process her measurement results. Consequently, the entire process Ξ transforms the initial assemblage $\sigma_{a|x}$ into a final assemblage $\sigma_{a'|x'}$:

$$\sigma_{a'|x'} = \Xi(\sigma_{a|x}) = \sum_{a, x, \xi} p(x|x', \xi) p(a'|a, x, x', \xi) p(\xi) \Xi_{\xi}(\sigma_{a|x}). \quad (28)$$

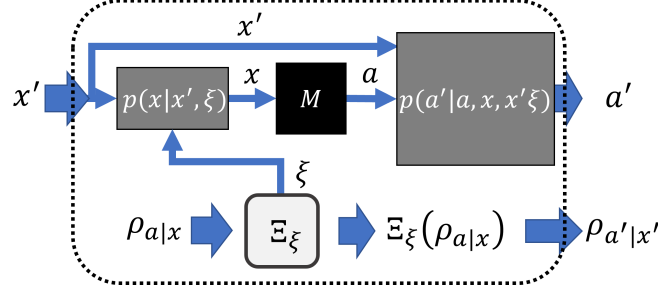


Figure 4. Schematic illustration of one-way local genuinely incoherent operations and classical communication. The final assemblage $\sigma_{a'|x'} = \Xi(\sigma_{a|x})$ is given by a black box (represented by black-dashed rectangle) with inputs x' and outputs a' . To do this, Bob first applied a genuinely incoherent operation Ξ_{ξ} with probability $p(\xi)$ on his subsystem $\rho_{a|x}$ and obtain the state $\rho_{a'|x'} = \Xi_{\xi}(\rho_{a|x})$. Thereafter, he send ξ to Alice through classical communication. Based on the information of x' and ξ , Alice performs a local wiring map (the first gray box) with probability distribution $p(x|x', \xi)$ generating inputs x for her measurements M . Then, Alice receives outcomes a and processes all classical labels a, x, x' , and ξ to generate the final outputs a' by a local wiring map (the second gray box) with a probability distribution $p(a'|a, x, x', \xi)$.

Now, we prove that the SIVP is monotonic under this constrain.

Proof. — We aim to use the strategy in Eqs. (44) and (45) by first showing that C_d^* is non-increasing after the process, namely

$$\begin{aligned} C_d^*[\Xi(\mathcal{A})] &= \max_{x'} \sum_{a'} p(a'|x') C_d \left[\frac{\sigma_{a'|x'}}{p(a'|x')} \right] \\ &= \max_{x'} \sum_{a'} p(a'|x') C_d \left[\sum_{a, x, \xi} \frac{p(x|x', \xi) p(a'|a, x, x', \xi) K_{\xi} \sigma_{a|x} K_{\xi}^{\dagger}}{p(a'|x')} \right] \\ &= \max_{x'} \sum_{a'} p(a'|x') C_d \left[\sum_{a, x, \xi} \frac{p(x|x', \xi)}{p(a'|x')} \frac{p(a'|a, \xi) p(x|a', x', \xi) p(a|x, a', x', \xi)}{p(x|x', \xi) p(a|x, x', \xi)} p(a|x) K_{\xi} \rho_{a|x} K_{\xi}^{\dagger} \right] \\ &= \max_{x'} \sum_{a'} p(a'|x') C_d \left[\sum_{a, x, \xi} \frac{p(a'|a, \xi) p(x|x', \xi)}{p(a'|x')} p(a|x) K_{\xi} \rho_{a|x} K_{\xi}^{\dagger} \right] \\ &= \max_{x'} \sum_{a'} p(a'|x') C_d \left[\sum_{a, x} p(x) p(a|x) \sum_{\xi} p(\xi) \Xi_{\xi}(\rho_{a|x}) \right] \\ &\leq \max_{x'} \sum_{a'} p(a'|x') \sum_{a, x} p(x) p(a|x) C_d \left(\sum_{\xi} p(\xi) \Xi_{\xi}(\rho_{a|x}) \right) \\ &\leq \sum_x p(x) \sum_a p(a|x) C_d \left(\sum_{\xi} p(\xi) \rho_{a|x} \right) \\ &\leq \max_x \sum_a p(a|x) C_d(\rho_{a|x}) \\ &= C_d^*(\mathcal{A}). \end{aligned} \quad (29)$$

Again, in the third line, we utilize the relation: $p(a'|a, x, x', \xi) = p(a'|x', \xi) p(x|a', x', \xi) p(a|x, a', x', \xi) / [p(x|x', \xi) p(a|x, x', \xi)]$. For the fourth line, the label x should not depend on a , and the label a should not depend on x' and a' , as shown in Fig. 4.

In the fifth line, we use the relation $p(x) = p(x|x', \xi)p(a'|a, x, x', \xi)/p(a'|x')$. In addition, we use the convexity of C_d and its monotonic property under incoherent operations to deduce the inequalities in the sixth and seventh lines, respectively.

In contrast, the H_Δ^* will always increase monotonically after the process:

$$\begin{aligned}
H_\Delta^*[\Xi(\mathcal{A})] &= \min_{x'} \sum_{a'} p(a'|x') H_\Delta \left[\frac{\sigma_{a'|x'}}{p(a'|x')} \right] \\
&= \min_{x'} \sum_{a'} p(a'|x') H_\Delta \left[\sum_{a,x,\xi} p(x)p(a|x)p(\xi) \Xi_\xi(\rho_{a|x}) \right] \\
&\geq \sum_{a,x} p(x)p(a|x) H_\Delta \left[\sum_{\xi} p(\xi) \Xi_\xi(\rho_{a|x}) \right] \\
&= \sum_x p(x) \sum_a p(a|x) H_\Delta \left[\sum_{\xi} p(\xi) \left(\sum_k K_{k,\xi} \rho_{a|x} K_{k,\xi}^\dagger \right) \right] \\
&= \sum_x p(x) \sum_a p(a|x) S \left[\sum_{i,k,\xi} p(\xi) |c_i^{k,\xi}|^2 \langle i | \rho_{a|x} | i \rangle | i \rangle \langle i | \right] \\
&= \sum_x p(x) \sum_a p(a|x) S[\Delta(\rho_{a|x})] \\
&\geq \min_x \sum_a p(a|x) H_\Delta(\rho_{a|x}) \\
&= H_\Delta^*(\mathcal{A}).
\end{aligned} \tag{30}$$

In this derivation, we use the concavity of the H_Δ and the definition of genuinely incoherent operations in Eq. (27). Therefore, by using a relation similar to Eq. (46), we can conclude that $\mathcal{V}_S(\mathcal{A}) \geq \mathcal{V}_S[\Xi(\mathcal{A})]$, which ends the proof. \square

One can observe that our proof strategy aims to demonstrate:

$$C_d^*(\mathcal{A}) - C_d^*[\Xi(\mathcal{A})] \geq 0 \geq H_\Delta^*(\mathcal{A}) - H_\Delta^*[\Xi(\mathcal{A})], \tag{31}$$

which offers a weaker validation of the relationship

$$C_d^*(\mathcal{A}) - H_\Delta^*(\mathcal{A}) \geq C_d^*[\Xi(\mathcal{A})] - H_\Delta^*[\Xi(\mathcal{A})]. \tag{32}$$

This is because any Ξ satisfying Eq. (31) automatically meets the conditions of Eq. (32). However, the converse is not necessarily true; that is, all Ξ that meet the conditions of Eq. (32) may not satisfy Eq. (31). To derive the former inequality, we must limit the local operations to genuinely incoherent operations, which form a subset of incoherent operations.

Numerical evidence for the monotonicity of the SIVP

We have numerically tested the monotonicity of the SIVP using 10^7 random pure entangled states ρ^{AB} and random local incoherent maps $\Lambda(\rho) = \sum_\mu K_\mu \rho K_\mu^\dagger$ on Bob's side by setting:

$$K_\mu = c_\mu |f_\mu(i)\rangle \langle i| \quad \text{s.t.} \quad K_\mu \rho K_\mu^\dagger \in \mathcal{I} \quad \forall \rho \in \mathcal{I} \quad \text{and} \quad \sum_\mu K_\mu^\dagger K_\mu = \mathbb{1}, \tag{33}$$

where $f_\mu(i)$ are arbitrary functions used to map one reference basis $|i\rangle$ into another reference basis $|f_\mu(i)\rangle$. For each pure entangled state, we assume that Alice performs the Pauli X (σ_1) and Z (σ_3) measurements, i.e., $M_{a|x} = [\mathbb{1} + (-1)^a \sigma_x]/2$, with $a \in \{0, 1\}$ and $x \in \{1, 3\}$. After receiving the assemblage $\mathcal{A} = \{\sigma_{a|x} = p(a|x)\rho_{a|x}\}_{a,x}$, Bob computes both $\mathcal{V}_S(\mathcal{A})$ and $\mathcal{V}_S[\Lambda(\mathcal{A})]$ under the reference basis $\{|i\rangle\}_{i=0,1}$ (eigenbasis of Pauli-Z). Out of all 10^7 random tests, we found that the SIVP always decreased after local incoherent maps. Therefore, we conclude from the numerical tests that the SIVP could be non-increasing under one-way local incoherent operations and classical communication⁵⁰.

Local CPTP maps, on the other hand, could increase the SIVP. Given that some CPTP maps may generate local coherence and are not belong to incoherent operations. For instance, consider the following state ρ^{AB} as

$$\rho^{AB} = \begin{pmatrix} 0.276 & 0.293 - 0.062i & -0.027 + 0.251i & 0.073 - 0.203i \\ 0.293 + 0.062i & 0.325 & -0.085 + 0.026i & 0.123 - 0.199i \\ -0.027 - 0.251i & -0.085 - 0.026i & 0.230 & -0.191 - 0.047i \\ 0.073 + 0.203i & 0.123 + 0.199i & -0.191 + 0.047i & 0.168 \end{pmatrix} \tag{34}$$

and a CPTP map: $\Lambda_1(\rho) = \sum_{i=0}^3 K_i \rho K_i^\dagger$ with the Kraus operators:

$$\begin{aligned} K_0 &= \begin{pmatrix} 0.559 + 0.351i & 0.425 - 0.487i \\ 0.721 & -0.024 + 0.564i \end{pmatrix}, & K_1 &= \begin{pmatrix} 0.004 + 0.021i & 0.388 \\ -0.160 - 0.030i & 0.319 - 0.091i \end{pmatrix}, \\ K_2 &= \begin{pmatrix} -0.050 - 0.071i & 0.032 + 0.020i \\ 0.097 & 0.005 - 0.037i \end{pmatrix}, & K_3 &= \begin{pmatrix} 0.021 & 0.006 + 0.012i \\ 0.001 - 0.012i & -0.013 - 0.016i \end{pmatrix}. \end{aligned} \quad (35)$$

By calculating the SIVPs, we obtain

$$\mathcal{V}_S(\mathcal{A}) \approx 0.061 \quad \text{and} \quad \mathcal{V}_S[\Lambda_1(\mathcal{A})] \approx 0.198, \quad (36)$$

which demonstrates that the SIVP increases after the CPTP map. However, when applying this map to a maximally mixed state $\mathbb{1}/2$, we find that

$$\Lambda_1\left(\frac{\mathbb{1}}{2}\right) = \begin{pmatrix} 0.506 & 0.117 + 0.026i \\ 0.117 - 0.026i & 0.494 \end{pmatrix}, \quad (37)$$

which implies that $\Lambda_1 \notin \text{ICO}$. In fact, $\Lambda_1[\rho_I(\alpha)] \notin \text{ICO} \forall \rho_I = \alpha|0\rangle\langle 0| + (1-\alpha)|1\rangle\langle 1| \in \mathcal{S} \forall \alpha \in [0, 1]$.

Proof that SIVP serves as an incompatibility monotone

$\mathcal{V}_I(\mathcal{M})$ is a valid incompatibility monotone⁵⁶ if it satisfies:

- (a) $\mathcal{V}_I(\mathcal{M}) = 0$, if \mathcal{M} is jointly measurable.
- (b) $\mathcal{V}_I(\mathcal{M})$ satisfies convexity.
- (c) $\mathcal{V}_I(\mathcal{M})$ is non-increasing under post-processing, namely

$$\{M_{a'|x'}\}_{a',x'} = \mathcal{W}(\{M_{a|x}\}_{a,x}) = \sum_{a,x} p(x|x') p(a'|a, x, x') \{M_{a|x}\}_{a,x}. \quad (38)$$

Proof of condition (a):

The condition (a) is automatically satisfied by the definition of \mathcal{V}_I :

$$\mathcal{V}_I(\{M_{a|x}\}_{a,x}) = \sup_{\rho_B} \mathcal{V}_S[\sqrt{\rho_B} \{M_{a|x}\}_{a,x} \sqrt{\rho_B}]. \quad (39)$$

Given that a set of measurements $\{M_{a|x}\}_{a,x}$ is compatible if and only if its steering-equivalent observables induced a state assemblage $\sqrt{\rho_B} \{M_{a|x}\}_{a,x} \sqrt{\rho_B}$ that can be described by an LHS model. Thus, the SIVP vanishes.

Proof of condition (b):

To prove that (b) $\mathcal{V}_I(\mathcal{M})$ satisfies convexity, we only need to demonstrate $\mathcal{V}_S(\mathcal{A})$ is convex in assemblage.

Let us consider a convex combination of the state assemblages that can be described by

$$\tilde{\mathcal{A}} = q\mathcal{A} + (1-q)\mathcal{A}' := \{q\sigma_{a|x} + (1-q)\sigma'_{a|x}\}_{a,x} \quad \forall q \in [0, 1]. \quad (40)$$

Using the convexity of C_d , one can obtain

$$\begin{aligned} C_d^*(\tilde{\mathcal{A}}) &= C_d^*[q\mathcal{A} + (1-q)\mathcal{A}'] \\ &= \max_x \sum_a p(a|x) C_d[q\rho_{a|x} + (1-q)\rho'_{a|x}] \\ &\leq \max_x \sum_a [qp(a|x)C_d(\rho_{a|x}) + (1-q)p'(a|x)C_d(\rho'_{a|x})] \\ &\leq q \max_x \sum_a p(a|x)C_d(\rho_{a|x}) + (1-q) \max_x \sum_a p'(a|x)C_d(\rho'_{a|x}) \\ &= qC_d^*(\mathcal{A}) + (1-q)C_d^*(\mathcal{A}'). \end{aligned} \quad (41)$$

Following the analogous steps, together with the fact that the Shannon entropy is concave, we can demonstrate that H_Δ^* is also concave with respect to a convex combination of the state assemblages. Therefore, we can conclude that the steering

violation satisfies convexity, namely

$$\begin{aligned}
\mathcal{V}_S(\mathcal{A}) &= \mathcal{V}_S[q\mathcal{A} + (1-q)\mathcal{A}'] \\
&= \max\{C_d^*[q\mathcal{A} + (1-q)\mathcal{A}'] - H_\Delta^*[q\mathcal{A} + (1-q)\mathcal{A}'], 0\} \\
&\leq \max\{q[C_d^*(\mathcal{A}) - H_\Delta^*(\mathcal{A})] + (1-q)[C_d^*(\mathcal{A}') - H_\Delta^*(\mathcal{A}')], 0\} \\
&\leq q \max\{C_d^*(\mathcal{A}) - H_\Delta^*(\mathcal{A}), 0\} + (1-q) \max\{C_d^*(\mathcal{A}') - H_\Delta^*(\mathcal{A}'), 0\} \\
&= q\mathcal{V}_S(\mathcal{A}) + (1-q)\mathcal{V}_S(\mathcal{A}').
\end{aligned} \tag{42}$$

Here, we use the facts that $C_d(H_\Delta^*)$ is a convex (concave) function and the property of the maximization in order. Therefore, we conclude the proof that $\mathcal{V}_1(\mathcal{M})$ satisfies convexity.

Proof of condition (c):

To prove that $\mathcal{V}_1(\mathcal{M})$ is non-increasing under post-processing, we consider a post-processing scenario \mathcal{W} defined as a deterministic wiring map⁴⁹, as shown in Fig. 5:

$$\sigma_{a'|x'} = \mathcal{W}(\sigma_{a|x}) = \sum_{a,x} p(x|x')p(a'|a,x,x')\sigma_{a|x}, \quad \forall a,x, \tag{43}$$

where $p(x|x')$ and $p(a'|a,x,x')$ are conditional probabilities. We first need to demonstrate that $\mathcal{V}_S(\mathcal{A})$ is also non-increasing

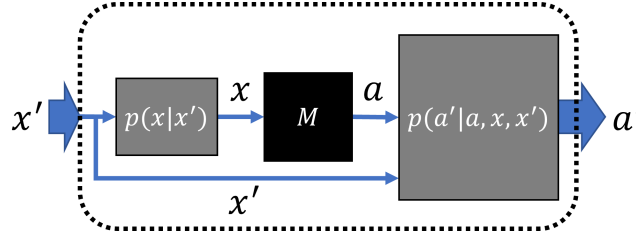


Figure 5. Schematic illustration of post-processing. See the caption in Fig. 4

under post-processing. We begin this proof by showing that C_d^* is non-increasing under post-processing, that is

$$\begin{aligned}
C_d^*[\mathcal{W}(\mathcal{A})] &= \max_{x'} \sum_{a'} p(a'|x') C_d \left[\frac{\sigma_{a'|x'}}{p(a'|x')} \right] \\
&= \max_{x'} \sum_{a'} p(a'|x') C_d \left[\sum_{a,x} \frac{p(x|x')p(a'|a,x,x')\sigma_{a|x}}{p(a'|x')} \right] \\
&= \max_{x'} \sum_{a'} p(a'|x') C_d \left[\sum_{a,x} \frac{p(x|x')}{p(a'|x')} \frac{p(a'|x')p(x|x')p(a|x,x')}{p(x|x')p(a|x,x')} p(a|x)\rho_{a|x} \right] \\
&= \max_{x'} \sum_{a'} p(a'|x') C_d \left[\sum_{a,x} \frac{p(x|x')}{p(a'|x')} \frac{p(a'|x')p(x|x')p(a|x,x')}{p(x|x')p(a|x,x')} p(a|x)\rho_{a|x} \right] \\
&= \max_{x'} \sum_{a'} p(a'|x') C_d \left[\sum_{a,x} \frac{p(a'|x')p(x|x')}{p(a'|x')} p(a|x)\rho_{a|x} \right] \\
&= \max_{x'} \sum_{a'} p(a'|x') C_d \left[\sum_{a,x} p(x)p(a|x)\rho_{a|x} \right] \\
&\leq \max_{x'} \sum_{a'} p(a'|x') \sum_{a,x} p(x)p(a|x) C_d(\rho_{a|x}) \\
&= \sum_x p(x) \sum_a p(a|x) C_d(\rho_{a|x}) \\
&\leq \max_x \sum_a p(a|x) C_d(\rho_{a|x}) \\
&= C_d^*(\mathcal{A}).
\end{aligned} \tag{44}$$

Here, we utilize the relation $p(a'|a, x, x') = p(a'|x')p(x|x', a')p(a|x, x', a')/[p(x|x')p(a|x, x')]$ to arrive at the equation in the third line; in the fourth line, we note that all the labels, say x, x', a should not depend on a' ; in the sixth line, we use the relation of $p(x|x') = p(x)p(x'|x)/p(x') = p(x)$, given that x' should not depend on x ; the seventh line uses the convexity of C_d .

In contrast, the conditional Shannon entropy increases monotonically after the process due to concavity, namely

$$\begin{aligned}
H_\Delta^*[\mathcal{W}(\mathcal{A})] &= \min_{x'} \sum_{a'} p(a'|x') H_\Delta \left[\frac{\sigma_{a'|x'}}{p(a'|x')} \right] \\
&= \min_{x'} \sum_{a'} p(a'|x') H_\Delta \left[\sum_{a,x} p(x)p(a|x)\rho_{a|x} \right] \\
&\geq \sum_{a,x} p(x)p(a|x) H_\Delta(\rho_{a|x}) \\
&\geq \min_x \sum_a p(a|x) H_\Delta(\rho_{a|x}) \\
&= H_\Delta^*(\mathcal{A}).
\end{aligned} \tag{45}$$

Combining the results in Eqs. (44) and (45), one can conclude that

$$C_d^*(\mathcal{A}) - C_d^*[\mathcal{W}(\mathcal{A})] \geq 0 \geq H_\Delta^*(\mathcal{A}) - H_\Delta^*[\mathcal{W}(\mathcal{A})], \tag{46}$$

which implies $\mathcal{V}_S(\mathcal{A}) \geq \mathcal{V}_S[\mathcal{W}(\mathcal{A})]$.

By using the above results, we can therefore show that $\mathcal{V}_I(\mathcal{M})$ is also non-increasing under post-processing, i.e.,

$$\begin{aligned}
\mathcal{V}_I[\mathcal{W}(\mathcal{M})] &= \sup_{\rho_B} \mathcal{V}_S[\sqrt{\rho_B} \mathcal{W}(\mathcal{M}) \sqrt{\rho_B}] \\
&= \mathcal{V}_S[\sqrt{\rho_B^*} \mathcal{W}(\mathcal{M}) \sqrt{\rho_B^*}] \\
&= \mathcal{V}_S[\mathcal{W}(\sqrt{\rho_B^*} \mathcal{M} \sqrt{\rho_B^*})] \\
&\leq \mathcal{V}_S(\sqrt{\rho_B^*} \mathcal{M} \sqrt{\rho_B^*}) \\
&\leq \sup_{\rho_B} \mathcal{V}_S(\sqrt{\rho_B} \mathcal{M} \sqrt{\rho_B}) \\
&= \mathcal{V}_I(\mathcal{M}).
\end{aligned} \tag{47}$$

Data availability

Dataset underlying the results presented in Fig. 2 is available in Ref.⁷¹.

Code availability

Source codes of the plots are available from the authors upon request.

Acknowledgments

We are grateful to Eric Chitambar for fruitful discussion. A.M. is supported by the Polish National Science Centre (NCN) under the Maestro Grant No. DEC-2019/34/A/ST2/00081. A.Č. and K.L. acknowledge support by the project OP JAC CZ.02.01.01/00/22_008/0004596 of the Ministry of Education, Youth, and Sports of the Czech Republic and EU. F.N. is supported in part by: Nippon Telegraph and Telephone Corporation (NTT) Research, the Japan Science and Technology Agency (JST) [via the Quantum Leap Flagship Program (Q-LEAP), and the Moonshot R&D Grant Number JPMJMS2061], the Asian Office of Aerospace Research and Development (AOARD) (via Grant No. FA2386-20-1-4069), and the Office of Naval Research (ONR) Global (via Grant No. N62909-23-1-2074). H.-Y. K. is supported by the Ministry of Science and Technology, Taiwan, (Grants No. MOST 111-2917-I-564-005, 112-2112-M-003 -020 -MY3), and Higher Education Sprout Project of National Taiwan Normal University (NTNU) and the Ministry of Education (MOE) in Taiwan. This work is supported by the National Center for Theoretical Sciences and National Science and Technology Council, Taiwan, Grants No. NSTC 112-2123-M-006-001.

Author contributions

K.-Y. L. and J.-D. L. contributed equally to this work. K.-Y. L. and J.-D. L. performed the computations and proved the properties with H.-Y. K.'s help. K. L. and A. Č designed the experimental setup and conducted the experiment; they analyzed the experimental data together with A. M. and K.-Y. L. K.-Y. L., J.-D. L., K. L., and H.-Y. K. contributed to analyzing the results and wrote the first draft of the manuscript. F. N., H.-Y. K. and Y.-N. C. supervised the research and were responsible for the integration among different research units. All authors contributed to the discussion of the central ideas and reviewed the manuscript.

Competing interests

The authors declare no competing interests.

References

1. Wiseman, H. M., Jones, S. J. & Doherty, A. C. Steering, entanglement, nonlocality, and the Einstein-Podolsky-Rosen paradox. *Phys. Rev. Lett.* **98**, 140402, DOI: <https://doi.org/10.1103/PhysRevLett.98.140402> (2007).
2. Piani, M. & Watrous, J. Necessary and sufficient quantum information characterization of Einstein-Podolsky-Rosen steering. *Phys. Rev. Lett.* **114**, 060404, DOI: <https://doi.org/10.1103/PhysRevLett.114.060404> (2015).
3. Lin, J.-D. *et al.* Quantum steering as a witness of quantum scrambling. *Phys. Rev. A* **104**, 022614, DOI: <https://doi.org/10.1103/PhysRevA.104.022614> (2021).
4. Huang, Y.-T., Lin, J.-D., Ku, H.-Y. & Chen, Y.-N. Benchmarking quantum state transfer on quantum devices. *Phys. Rev. Res.* **3**, 023038, DOI: <https://doi.org/10.1103/PhysRevResearch.3.023038> (2021).
5. Ku, H.-Y. *et al.* Quantifying quantumness of channels without entanglement. *PRX Quantum* **3**, 020338, DOI: <https://doi.org/10.1103/PRXQuantum.3.020338> (2022).
6. Ku, H.-Y., Lee, K.-Y., Lai, P.-R., Lin, J.-D. & Chen, Y.-N. Coherent activation of a steerability-breaking channel. *Phys. Rev. A* **107**, 042415, DOI: <https://doi.org/10.1103/PhysRevA.107.042415> (2023).
7. Skrzypczyk, P. & Cavalcanti, D. Maximal randomness generation from steering inequality violations using qubits. *Phys. Rev. Lett.* **120**, 260401, DOI: <https://doi.org/10.1103/PhysRevLett.120.260401> (2018).
8. Guo, Y. *et al.* Experimental measurement-device-independent quantum steering and randomness generation beyond qubits. *Phys. Rev. Lett.* **123**, 170402, DOI: <https://doi.org/10.1103/PhysRevLett.123.170402> (2019).
9. Branciard, C., Cavalcanti, E. G., Walborn, S. P., Scarani, V. & Wiseman, H. M. One-sided device-independent quantum key distribution: Security, feasibility, and the connection with steering. *Phys. Rev. A* **85**, 010301(R) (2012).
10. Bartkiewicz, K., Černoč, A., Lemr, K., Miranowicz, A. & Nori, F. Temporal steering and security of quantum key distribution with mutually unbiased bases against individual attacks. *Phys. Rev. A* **93**, 062345, DOI: <https://doi.org/10.1103/PhysRevA.93.062345> (2016).
11. Yadin, B., Fadel, M. & Gessner, M. Metrological complementarity reveals the Einstein-Podolsky-Rosen paradox. *Nat. Commun.* **12**, 2410, DOI: <https://doi.org/10.1038/s41467-021-22353-3> (2021).
12. Lee, K.-Y. *et al.* Steering-enhanced quantum metrology using superpositions of noisy phase shifts. *Phys. Rev. Res.* **5**, 013103, DOI: <https://doi.org/10.1103/PhysRevResearch.5.013103> (2023).
13. Hsieh, C.-Y. & Chen, S.-L. A thermodynamic approach to quantifying incompatible instruments. *arXiv e-prints* arXiv:2402.13080, DOI: <https://doi.org/10.48550/arXiv.2402.13080> (2024). [2402.13080](https://arxiv.org/abs/2402.13080).
14. Hsieh, C.-Y. & Gessner, M. General quantum resources provide advantages in work extraction tasks. *arXiv e-prints* arXiv:2403.18753, DOI: <https://doi.org/10.48550/arXiv.2403.18753> (2024). [2403.18753](https://arxiv.org/abs/2403.18753).
15. Cavalcanti, D. & Skrzypczyk, P. Quantum steering: a review with focus on semidefinite programming. *Reports on Prog. Phys.* **80**, 024001, DOI: <https://doi.org/10.1088/1361-6633/80/2/024001> (2016).
16. Uola, R., Costa, A. C. S., Nguyen, H. C. & Gühne, O. Quantum steering. *Rev. Mod. Phys.* **92**, 015001, DOI: <https://doi.org/10.1103/RevModPhys.92.015001> (2020).
17. Xiang, Y., Cheng, S., Gong, Q., Ficek, Z. & He, Q. Quantum steering: Practical challenges and future directions. *PRX Quantum* **3**, 030102, DOI: <https://doi.org/10.1103/PRXQuantum.3.030102> (2022).
18. Reid, M. D. Demonstration of the Einstein-Podolsky-Rosen paradox using nondegenerate parametric amplification. *Phys. Rev. A* **40**, 913–923, DOI: <https://doi.org/10.1103/PhysRevA.40.913> (1989).
19. Reid, M. D. *et al.* Colloquium: The Einstein-Podolsky-Rosen paradox: From concepts to applications. *Rev. Mod. Phys.* **81**, 1727–1751, DOI: <https://doi.org/10.1103/RevModPhys.81.1727> (2009).
20. Deutsch, D. Uncertainty in quantum measurements. *Phys. Rev. Lett.* **50**, 631–633, DOI: [10.1103/PhysRevLett.50.631](https://doi.org/10.1103/PhysRevLett.50.631) (1983).

21. Maassen, H. & Uffink, J. B. M. Generalized entropic uncertainty relations. *Phys. Rev. Lett.* **60**, 1103–1106, DOI: <https://doi.org/10.1103/PhysRevLett.60.1103> (1988).
22. Coles, P. J., Berta, M., Tomamichel, M. & Wehner, S. Entropic uncertainty relations and their applications. *Rev. Mod. Phys.* **89**, 015002, DOI: <https://doi.org/10.1103/RevModPhys.89.015002> (2017).
23. Karthik, H., Usha Devi, A., Prabhu Tej, J. & Rajagopal, A. Conditional entropic uncertainty and quantum correlations. *Opt. Commun.* **427**, 635–640, DOI: <https://doi.org/10.1016/j.optcom.2018.07.006> (2018).
24. Mondal, D., Pramanik, T. & Pati, A. K. Nonlocal advantage of quantum coherence. *Phys. Rev. A* **95**, 010301(R), DOI: <https://doi.org/10.1103/PhysRevA.95.010301> (2017).
25. Hu, M.-L. & Fan, H. Nonlocal advantage of quantum coherence in high-dimensional states. *Phys. Rev. A* **98**, 022312, DOI: <https://doi.org/10.1103/PhysRevA.98.022312> (2018).
26. Quintino, M. T., Vértesi, T. & Brunner, N. Joint measurability, Einstein-Podolsky-Rosen steering, and Bell nonlocality. *Phys. Rev. Lett.* **113**, 160402, DOI: <https://doi.org/10.1103/PhysRevLett.113.160402> (2014).
27. Uola, R., Moroder, T. & Gühne, O. Joint measurability of generalized measurements implies classicality. *Phys. Rev. Lett.* **113**, 160403, DOI: <https://doi.org/10.1103/PhysRevLett.113.160403> (2014).
28. Uola, R., Budroni, C., Gühne, O. & Pellonpää, J.-P. One-to-one mapping between steering and joint measurability problems. *Phys. Rev. Lett.* **115**, 230402, DOI: <https://doi.org/10.1103/PhysRevLett.115.230402> (2015).
29. Cavalcanti, D. & Skrzypczyk, P. Quantitative relations between measurement incompatibility, quantum steering, and nonlocality. *Phys. Rev. A* **93**, 052112, DOI: <https://doi.org/10.1103/PhysRevA.93.052112> (2016).
30. Zhao, Y.-Y. *et al.* Experimental demonstration of measurement-device-independent measure of quantum steering. *npj Quantum Inf.* **6**, 77, DOI: <https://doi.org/10.1038/s41534-020-00307-9> (2020).
31. Wang, H.-M., Ku, H.-Y., Lin, J.-Y. & Chen, H.-B. Deep learning the hierarchy of steering measurement settings of qubit-pair states. *Commun. Phys.* **7**, 72, DOI: <https://doi.org/10.1038/s42005-024-01563-3> (2024).
32. Luo, S. Wigner-Yanase skew information and uncertainty relations. *Phys. Rev. Lett.* **91**, 180403, DOI: <https://doi.org/10.1103/PhysRevLett.91.180403> (2003).
33. Luo, S. L. Quantum versus classical uncertainty. *Theor. Math. Phys.* **143**, 681–688, DOI: <https://doi.org/10.1007/s11232-005-0098-6> (2005).
34. Korzekwa, K., Lostaglio, M., Jennings, D. & Rudolph, T. Quantum and classical entropic uncertainty relations. *Phys. Rev. A* **89**, 042122, DOI: <https://doi.org/10.1103/PhysRevA.89.042122> (2014).
35. Yuan, X., Bai, G., Peng, T. & Ma, X. Quantum uncertainty relation using coherence. *Phys. Rev. A* **96**, 032313, DOI: <https://doi.org/10.1103/physreva.96.032313> (2017).
36. Hall, M. J. W. Asymmetry and tighter uncertainty relations for rényi entropies via quantum-classical decompositions of resource measures. *Phys. Rev. A* **107**, 062215, DOI: <https://doi.org/10.1103/physreva.107.062215> (2023).
37. Winter, A. & Yang, D. Operational resource theory of coherence. *Phys. Rev. Lett.* **116**, 120404, DOI: <https://doi.org/10.1103/PhysRevLett.116.120404> (2016).
38. Baumgratz, T., Cramer, M. & Plenio, M. B. Quantifying coherence. *Phys. Rev. Lett.* **113**, 140401, DOI: <https://doi.org/10.1103/PhysRevLett.113.140401> (2014).
39. Sun, Y. & Luo, S. Coherence as uncertainty. *Phys. Rev. A* **103**, 042423, DOI: <https://doi.org/10.1103/PhysRevA.103.042423> (2021).
40. Girolami, D., Tufarelli, T. & Adesso, G. Characterizing nonclassical correlations via local quantum uncertainty. *Phys. Rev. Lett.* **110**, 240402, DOI: <https://doi.org/10.1103/PhysRevLett.110.240402> (2013).
41. Girolami, D. Observable measure of quantum coherence in finite dimensional systems. *Phys. Rev. Lett.* **113**, 170401, DOI: <https://doi.org/10.1103/PhysRevLett.113.170401> (2014).
42. Dressel, J. & Nori, F. Certainty in Heisenberg’s uncertainty principle: Revisiting definitions for estimation errors and disturbance. *Phys. Rev. A* **89**, 022106, DOI: <https://doi.org/10.1103/PhysRevA.89.022106> (2014).
43. Angelo, R. M. & Ribeiro, A. D. Wave-particle duality: An information-based approach. *Found. Phys.* **45**, 1407–1420, DOI: <https://doi.org/10.1007/s10701-015-9913-6> (2015).
44. Bowles, J., Vértesi, T., Quintino, M. T. & Brunner, N. One-way Einstein-Podolsky-Rosen steering. *Phys. Rev. Lett.* **112**, 200402, DOI: <https://doi.org/10.1103/PhysRevLett.112.200402> (2014).
45. Bowles, J., Hirsch, F., Quintino, M. T. & Brunner, N. Sufficient criterion for guaranteeing that a two-qubit state is unsteerable. *Phys. Rev. A* **93**, 022121, DOI: <https://doi.org/10.1103/PhysRevA.93.022121> (2016).
46. Skrzypczyk, P., Navascués, M. & Cavalcanti, D. Quantifying einstein-podolsky-rosen steering. *Phys. Rev. Lett.* **112**, 180404, DOI: <https://doi.org/10.1103/PhysRevLett.112.180404> (2014).
47. Hsieh, C.-Y., Liang, Y.-C. & Lee, R.-K. Quantum steerability: Characterization, quantification, superactivation, and unbounded amplification. *Phys. Rev. A* **94**, 062120, DOI: <https://doi.org/10.1103/PhysRevA.94.062120> (2016).

48. Ku, H.-Y. *et al.* Einstein-Podolsky-Rosen steering: Its geometric quantification and witness. *Phys. Rev. A* **97**, 022338, DOI: <https://doi.org/10.1103/PhysRevA.97.022338> (2018).
49. Gallego, R. & Aolita, L. Resource theory of steering. *Phys. Rev. X* **5**, 041008, DOI: <https://doi.org/10.1103/PhysRevX.5.041008> (2015).
50. Chitambar, E. *et al.* Assisted distillation of quantum coherence. *Phys. Rev. Lett.* **116**, 070402, DOI: <https://doi.org/10.1103/PhysRevLett.116.070402> (2016).
51. Yadin, B., Ma, J., Girolami, D., Gu, M. & Vedral, V. Quantum processes which do not use coherence. *Phys. Rev. X* **6**, 041028, DOI: <https://doi.org/10.1103/PhysRevX.6.041028> (2016).
52. Regula, B., Fang, K., Wang, X. & Adesso, G. One-shot coherence distillation. *Phys. Rev. Lett.* **121**, 010401, DOI: <https://doi.org/10.1103/PhysRevLett.121.010401> (2018).
53. Regula, B., Lami, L. & Streltsov, A. Nonasymptotic assisted distillation of quantum coherence. *Phys. Rev. A* **98**, 052329, DOI: <https://doi.org/10.1103/PhysRevA.98.052329> (2018).
54. Fang, K., Wang, X., Lami, L., Regula, B. & Adesso, G. Probabilistic distillation of quantum coherence. *Phys. Rev. Lett.* **121**, 070404, DOI: <https://doi.org/10.1103/PhysRevLett.121.070404> (2018).
55. Shiraishi, N. & Takagi, R. Arbitrary amplification of quantum coherence in asymptotic and catalytic transformation. *Phys. Rev. Lett.* **132**, 180202, DOI: <https://doi.org/10.1103/PhysRevLett.132.180202> (2024).
56. Skrzypczyk, P., Šupić, I. & Cavalcanti, D. All sets of incompatible measurements give an advantage in quantum state discrimination. *Phys. Rev. Lett.* **122**, 130403, DOI: <https://doi.org/10.1103/PhysRevLett.122.130403> (2019).
57. Buscemi, F., Chitambar, E. & Zhou, W. Complete resource theory of quantum incompatibility as quantum programmability. *Phys. Rev. Lett.* **124**, 120401, DOI: <https://doi.org/10.1103/PhysRevLett.124.120401> (2020).
58. Buscemi, F., Kobayashi, K., Minagawa, S., Perinotti, P. & Tosini, A. Unifying different notions of quantum incompatibility into a strict hierarchy of resource theories of communication. *Quantum* **7**, 1035, DOI: <https://doi.org/10.22331/q-2023-06-07-1035> (2023).
59. Buscemi, F. All entangled quantum states are nonlocal. *Phys. Rev. Lett.* **108**, 200401, DOI: <https://doi.org/10.1103/PhysRevLett.108.200401> (2012).
60. Brunner, N., Cavalcanti, D., Pironio, S., Scarani, V. & Wehner, S. Bell nonlocality. *Rev. Mod. Phys.* **86**, 419–478, DOI: <https://doi.org/10.1103/RevModPhys.86.419> (2014).
61. Budroni, C., Cabello, A., Gühne, O., Kleinmann, M. & Larsson, J.-A. Kochen-specker contextuality. *Rev. Mod. Phys.* **94**, 045007, DOI: <https://doi.org/10.1103/RevModPhys.94.045007> (2022).
62. Busch, P., Lahti, P. & Werner, R. F. Colloquium: Quantum root-mean-square error and measurement uncertainty relations. *Rev. Mod. Phys.* **86**, 1261–1281, DOI: <https://doi.org/10.1103/RevModPhys.86.1261> (2014).
63. Gühne, O., Haapasalo, E., Kraft, T., Pellonpää, J.-P. & Uola, R. Colloquium: Incompatible measurements in quantum information science. *Rev. Mod. Phys.* **95**, 011003, DOI: <https://doi.org/10.1103/RevModPhys.95.011003> (2023).
64. Hsieh, C.-Y., Ku, H.-Y. & Budroni, C. Characterisation and fundamental limitations of irreversible stochastic steering distillation. *arXiv.2309.06191* (2023).
65. Ku, H.-Y., Hsieh, C.-Y. & Budroni, C. Measurement incompatibility cannot be stochastically distilled. *arXiv.2308.02252* (2023).
66. Kwiat, P. G., Waks, E., White, A. G., Appelbaum, I. & Eberhard, P. H. Ultrabright source of polarization-entangled photons. *Phys. Rev. A* **60**, R773–R776, DOI: <https://doi.org/10.1103/PhysRevA.60.R773> (1999).
67. Halenková, E., Černoč, A., Lemr, K., Soubusta, J. & Drusová, S. Experimental implementation of the multifunctional compact two-photon state analyzer. *Appl. Opt.* **51**, 474–478, DOI: <https://doi.org/10.1364/AO.51.000474> (2012).
68. Ježek, M., Fiurášek, J. & Hradil, Z. Quantum inference of states and processes. *Phys. Rev. A* **68**, 012305, DOI: <https://doi.org/10.1103/PhysRevA.68.012305> (2003).
69. Zhao, Q., Liu, Y., Yuan, X., Chitambar, E. & Winter, A. One-shot coherence distillation: Towards completing the picture. *IEEE Transactions on Inf. Theory* **65**, 6441–6453, DOI: <https://doi.org/10.1109/TIT.2019.2911102> (2019).
70. Chitambar, E. Dephasing-covariant operations enable asymptotic reversibility of quantum resources. *Phys. Rev. A* **97**, 050301(R), DOI: <https://doi.org/10.1103/PhysRevA.97.050301> (2018).
71. Lemr, K., Antonin, C., Lee, K.-Y. & Miranowicz, A. Dataset 1, DOI: <https://doi.org/10.6084/m9.figshare.26074909.v2> (2024).